

STABLESEMANTICS: A SYNTHETIC LANGUAGE-VISION DATASET OF DENSE SEMANTIC REPRESENTATIONS IN NATURALISTIC IMAGES

Anonymous authors

Paper under double-blind review

ABSTRACT

Understanding dense visual semantics remains a fundamental challenge in computer vision, as semantically similar objects can exhibit drastically different visual appearances. Recent advancements in generative text-to-image frameworks have led to models that implicitly capture natural scene statistics. These models learn to model complex relationships between objects, lighting, and other visual factors, enabling the generation of detailed and contextually rich images from text captions. To advance visual semantic understanding and develop more robust and interpretable vision models, we present **StableSemantics**, a large-scale dataset composed of 224 thousand human-curated prompts, processed natural language captions, over 2 million synthetic images, and 10 million attention maps. The dataset provides fine-grained semantic attributions at the noun-chunk level, leverages human-generated prompts that correspond to visually interesting stable diffusion generations, and provides 10 generations per phrase, with cross-attention maps corresponding to noun chunks for each image. We explore the semantic distribution of generated images, examine the distribution of objects within images, and benchmark captioning and open vocabulary segmentation methods on our data. As the first diffusion dataset to include dense attention attributions, we expect StableSemantics to catalyze advances in visual semantic understanding and provide a foundation for developing more sophisticated and effective visual models.

1 INTRODUCTION

Dense visual scene understanding is a complex task that requires the integration of cues, context, and prior knowledge to navigate the inherent variability and complexity of the visual world. This complexity is particularly evident when considering the diversity of visual appearances that can correspond to a single semantic concept. For instance, entities that correspond to “man-made structures” can have vastly different visual appearances, ranging from sleek skyscrapers to rustic cottages. Similarly, objects that serve the same purpose, such as “containers,” can have diverse shapes, sizes, and materials. This disconnect between semantic meaning and visual appearance poses a significant challenge for computer vision systems (Brust & Denzler, 2018; Duan & Kuo, 2021; Alqasrawi, 2016; Barz & Denzler, 2020), requiring the disentanglement of the underlying semantic structure from visual differences (Caron et al., 2021; Xu et al., 2023; Elharrouss et al., 2021; VS et al., 2024; Hu et al., 2023; Quinn et al., 2017). To overcome this challenge, recent advances have adopted data-driven approaches, which learn to recognize patterns and relationships in large datasets of images and annotations. However, the reliance on large datasets of images and annotations poses a significant challenge in the development of segmentation models. Acquiring and annotating such datasets can be a time-consuming and resource-intensive process, requiring careful consideration of data quality and diversity.

This limitation has sparked interest in exploring alternative approaches that can reduce the need for large human-annotated datasets. One promising direction is the use of generative models, which have shown impressive results in translating between semantic meaning and visual appearance (Rombach et al., 2022; Podell et al., 2023; Song et al., 2020; Ho et al., 2022). In particular, diffusion-based text-to-image synthesis models have demonstrated an impressive ability to generate highly realistic images from textual descriptions, suggesting that these models must possess an implicit understanding of the

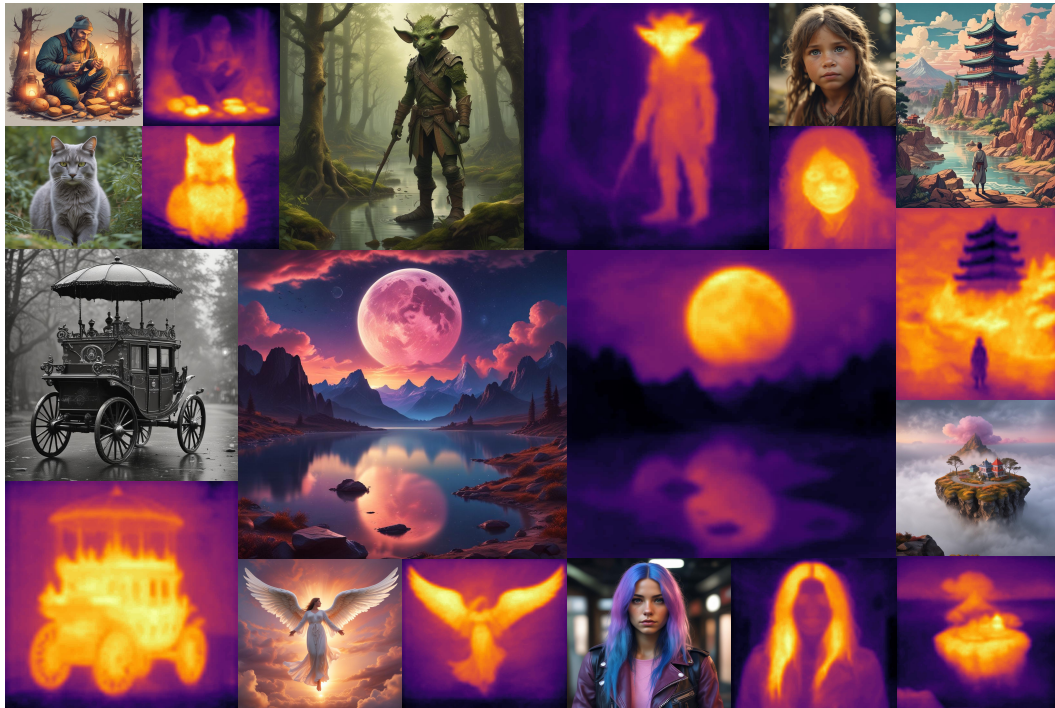


Figure 1: **Images and maps corresponding to select noun chunks from StableSemantics.** Images are generated using natural language captions derived from human generated and curated prompts. For reproducibility, seeds are recorded for each generation. Noun chunks are extracted by performing dependency parsing the natural language captions. Semantic maps corresponding to each noun chunk is computed using the cross-attention maps with the DAAM Tang et al. (2022) method. Only a single attention map is shown here for each image, please see below for additional examples. Yellow indicates high relevance, black indicates low relevance.

semantic structure of the visual world, and have learned to associate words and phrases with specific visual concepts. By leveraging cross-attention mechanisms, these models learn to link textual input to visual representations and enable the generation of images that are grounded in the semantic content of the input text (Tang et al., 2022). This in turn has led to generative media proliferating over social media, advertisements, and news media. Although generated images may seem indistinguishable from real images to the human eye, neural networks can still differentiate between them (Huang et al., 2024; Aziz et al., 2024; You et al., 2024). This suggests that generated images are still quite different from real images and that generative models are still far from perfect in accurately replicating the real data distribution (You et al., 2024). This demonstrates that a very clear gap still exists between generated and real data. Thus, there is a strong need for the development of more advanced generated data to help models perform well on synthetically generated images and to address the difficulty of gathering large-scale real data. Specifically, there are no existing large-scale generated datasets that contribute semantic maps in addition to images and their corresponding captions.

In this work, we introduce **StableSemantics**, a dataset that consists of human-generated and curated prompts, natural language captions, images generated from the captions, and attention attribution maps corresponding to objects in the captions. Unlike prior work which sourced unfiltered human-generated prompts, we source our prompts from a pool of images that have been evaluated by humans for their visual appeal and interest, resulting in a dataset that mirrors the types of images people find engaging. As the original prompts may not always reflect natural language, we employ a large language model to paraphrase and refine them into fluent and natural-sounding captions, thereby bridging the gap between human-generated prompts filtered for visual appeal and naturalistic language. Each natural language caption is provided to a Stable Diffusion XL model to generate high-resolution and reproducible images. Finally, we explicitly record the dense text-to-image cross-attention maps used to condition the image generation process. We visualize the distribution of semantics across images, evaluate the spatial distribution of semantic classes within images, and evaluate the alignment

of current captioning and open-set segmentation models on our dataset. To our knowledge, our dataset is the first to systematically record the spatial distribution of cross-attention activations corresponding to individual noun chunks. **StableSemantics** can be utilized in future research on various vision tasks such as object detection, semantic segmentation, semantically meaningful representation learning, image-inpainting and object removal, object editing, etc.

2 RELATED WORK

Natural Scene Statistics. Natural image statistics have been a long-standing area of research in computer vision and neuroscience. The human visual system is thought to be adapted to the statistical properties of natural images, which are characterized by complex dependencies between pixels (Girshick et al., 2011; van der Schaaf & van Hateren, 1996). The power law distribution of gradient magnitude statistics is thought to be a result of the hierarchical, self-similar structure of natural images, which arises from the presence of edges, textures, and other features at multiple scales. Understanding natural image statistics has important implications for image recognition tasks (Zoran, 2013; Heiler & Schnörr, 2005; Fang et al., 2012), and has inspired the development of a range of algorithms and models that are tailored to the statistical properties of natural images (Mechrez et al., 2019; Kleinlein et al., 2022; Hepburn et al., 2023; Xiang et al., 2024; Hepburn et al., 2021; Talbot et al., 2023). Other work has also explored the semantic structure of visual data, seeking to understand how higher-level categories and concepts are reflected in the statistical patterns present in images. This work has shown that different categories of images, such as scenes and objects, exhibit distinct statistical patterns (Torralba & Oliva, 2003; Henderson et al., 2023). These semantic statistics have important implications for the development of models that can effectively represent and analyze visual data.

Deep Image Generative Models. Recent progress on generative models has enabled the generation of images, video, text, and audio (Podell et al., 2023; Song et al., 2020; Ho et al., 2022; Gupta et al., 2023; Touvron et al., 2023; Evans et al., 2024). Models rely on a variety of different mathematical assumptions and architectures. Variational autoencoders (Kingma & Welling, 2013; Luhman & Luhman, 2023; Harvey et al., 2021; Razavi et al., 2019; Van Den Oord et al., 2017) and flow-based models (Rezende & Mohamed, 2015; Tong et al., 2023; Dinh et al., 2014; Kingma & Dhariwal, 2018), while highly efficient, tend to produce lower-quality samples. Generative Adversarial Networks (GANs) can yield high-fidelity samples but may neglect modes in the data and can exhibit unstable training dynamics (Goodfellow et al., 2014; Karras et al., 2019; Brock et al., 2018; Mirza & Osindero, 2014; Zawar et al., 2022). Auto-regressive methods (Huang et al., 2023; Parmar et al., 2018; Lee et al., 2022; Ramesh et al., 2022), although capable of producing high-quality samples, typically experience slow sampling. Recent progress in energy/score/diffusion models has given us methods that are simultaneously stable during training and yield high-quality samples (Rombach et al., 2022; Ramesh et al., 2022).

Visual Datasets. Deep learning models have achieved remarkable results by leveraging vast amounts of data. There has been a significant push to collect large-scale datasets. Earlier works such as LAION-5B (Schuhmann et al., 2022), Flickr Caption (Young et al., 2014), RedCaps (Desai et al., 2021) and YFCC100M (Thomee et al., 2016) scrape real-world data of image-caption pairs from web sources. COCO (Lin et al., 2014) goes a step further to also provide pixel-level segmentation masks on top of the image-caption pairs. (Agrawal et al., 2015; Goyal et al., 2016; Marino et al., 2019; Wang et al., 2018; Krishna et al., 2017) introduce datasets specifically for the task of VQA. Given the difficulty of collecting real data, recently there has been a shift towards synthetic datasets. StableRep (Tian et al., 2024) and Hammoud et al. (2024) also demonstrated the usefulness of Stable Diffusion images in training contrastive image models. Pick-a-Pic (Kirstain et al., 2023) provides a dataset of image-caption pairs where each sample contains a pair of diffusion-generated images and the human preference between those images. JourneyDB (Sun et al., 2023) and DiffusionDB (Wang et al., 2022b) are the closest works to ours that release large-scale datasets of synthetic image-caption pairs.

3 DATA COLLECTION

In this section, we provide details on the collection and creation process of our dataset. Our data originates from human-generated and curated prompts submitted publicly by users online for Stable Diffusion XL. We describe our prompt collection process in section 3.1. The prompts are filtered and transformed into natural language captions, and we describe our procedure in section 3.2. Finally, we generate images and compute noun-chunk to image saliency maps via cross-attention in section 3.3.

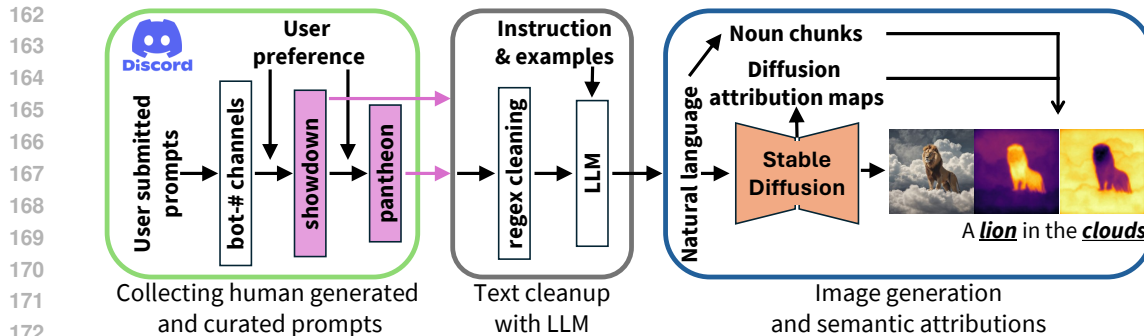


Figure 2: **Data collection and generation process.** (1) We collect our data from Stable Diffusion Discord, specifically the *showdown* and *pantheon* channels which are derived from user rankings of images generated from public prompt submissions. (2) The prompts are cleaned using regex to remove common errors, and further processed using an LLM to generate natural language captions. (3) The natural language captions are provided to a Stable Diffusion XL model, while we record the attention attribution maps corresponding to noun chunks.

3.1 COLLECTING HUMAN CURATED PROMPTS

Our dataset is collected from the *Stable Diffusion* discord server, where users can publicly submit prompts to generate images using a discord bot. After users submitted prompts using the `/dream` command, the bot would return images corresponding to a prompt. Beyond accepting a prompt, users could also submit negative prompts, and image styles which were achieved via a prefix/affix pattern of text to the original prompt. These style patterns were not visible to the users.

We started our data collection after the Stable Diffusion XL 1.0 (Podell et al., 2023) candidate was made available via bots. The data was continuously collected from **July 11, 2023** (a day after SDXL 1.0 candidate bots were launched) until **Feb 07, 2024** (SDXL bot shutdown). Users were allowed to submit prompts to `bot-#` channels where `#` corresponds to a number. We observed that the number of channels varied over time, and generally remained at slightly over 10. For each prompt, the bot would return 2 images. Users were asked to select which image was better by clicking on a button corresponding to an image, without explicit guidance on what "better" meant. Our understanding from discussions with members of staff was that these prompts and image pairs were used for fine-tuning the SDXL candidates using RLHF/DPO (Ouyang et al., 2022; Rafailov et al., 2024), selection of model candidates, and selection of generation hyperparameters.

Prior work has also collected user-generated prompts from discord servers for MidJourney and Stable Diffusion (Sun et al., 2023; Wang et al., 2022b). Our work goes further by only collecting prompts that were human-curated. The Stable Diffusion discord followed a three-tier hierarchy for prompts, where users first submit and rate images in `bot-#`, with highly rated images from all bot channels going into a single `showdown` channel every 15 minutes. The `showdown` channel was reset every 30 minutes and had the history wiped. In the `showdown` channel, 2 images and their respective prompts were placed side-by-side. Users again were asked to select the images that were more visually appealing. Every 30 minutes, the top-ranked images and prompts would go into the `pantheon` channel. The `pantheon` had history going back to inception May 02, 2023. We note that strictly speaking the `showdown` to `pantheon` selection process was not fair to images that came in at the second 15 minute slice, as they were given less time to be voted upon. Due to this, we do not further distinguish between prompts collected from these two sources. Our data collection process ran every 14 minutes on the `showdown` channels and ran once on the `pantheon` channel. This was sufficient as after the initial collection date, new `pantheon` entries were a strict subset of `showdown` prompts. Visual inspection of the generations from `showdown` and `pantheon` suggest that these images were generally more artistic and contained more interesting visual compositions than the `bot-#` channel. We collect a total of 235k unique user-generated prompts, which is further filtered according to NSFW ratings and caption length.

Dataset	Total Images	Total Captions	Caption Source	Human Preferred	Open-set Semantics
COCO 2017 Lin et al. (2014)	123k	617k	H	N	N
LAION-COCO Schuhmann et al. (2022)	600M	600M	M	N	N
DiffusionDB Wang et al. (2022b)	14M	1.8M	H	N	N
JourneyDB Sun et al. (2023)	4.7M	1.7M	H+M	N	N
StableSemantics	2M	224k	H+M	Y	10.8M

Table 1: **Size of the different components of StableSemantics.** Our captions are selected by humans to correspond to visually interesting images. We are the only dataset to provide dense open-set spatial semantic maps. Our maps are derived from the cross-attention maps in Stable prompts. Note that 235k unique captions are collected, 224k remain after NSFW filtering and only 200k captions are used for image generation after filtering for length.

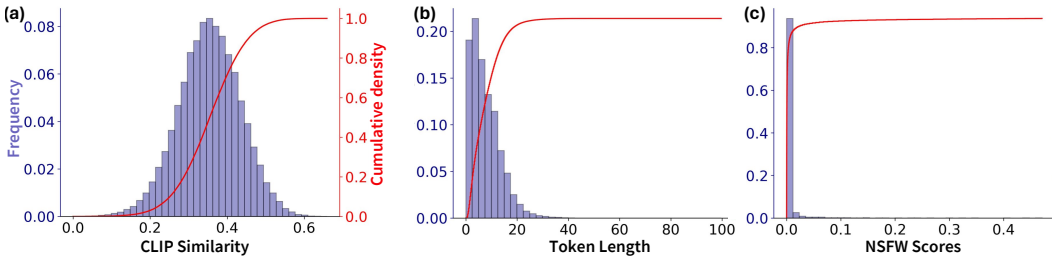


Figure 3: **Histogram of dataset statistics.** (a) We visualize the cosine CLIP similarities between generated images and original captions. (b) Number of tokens in the captions. (c) NSFW scores of the captions after LLM filtering. Scores measured by LLaMA Guard 2 for sexuality and hate.

3.2 OBTAINING NATURAL LANGUAGE CAPTIONS

As shown in Figure 4, the user-submitted prompts generally took a tag-like format, with descriptors being separated by commas. Such prompts are convenient for users to specify and likely achieve good results due to the use of CLIP text networks for conditioning, which can operate like bag-of-words models (Thrush et al., 2022; Yuksekogonul et al., 2022). However, such prompts generally perform poorly when typical NLP pipelines are used for analysis. These prompts further may not explicitly specify needed visual relationships in the text, and instead excessively rely on the prior learned by the diffusion model to disambiguate relationships. In order to mitigate this issue, we utilize an LLM model to clean up the original raw user-generated prompts. We use Gemini 1.0 Pro for this task, as it performed competitively against other models at the time of our work (Team et al., 2023) and offered a free API. The model was instructed to take the user-generated prompts and transform them into natural language captions. To enhance the results, we augment the prompt via in-context learning from GPT-4 input/output pairs. To remove NSFW prompts, we record the Gemini API safety ratings for each input prompt, and remove the prompts where a 4 out of 4 rating was given on the axes of sexuality/hate speech/harassment, or if the model itself produced a refusal, or if the prompt was repeatedly returned with an error (blocked by Google). Please see Figure 2 for a visualization of the pipeline.

3.3 IMAGE GENERATION AND SEMANTIC ATTRIBUTION

To provide a fully reproducible pipeline for the images and maximize the usability of our dataset, we generate the images ourselves using open weights and record the random seed for each generation. Images are generated using `sdxl lightning 4step unet` (Lin et al., 2024), a few-step distilled version of Stable Diffusion XL. For each prompt, we perform parsing using `spaCy en_core_web_lg` to extract noun chunks. To obtain mappings from noun chunks to spatial attributions, we use Diffusion Attentive Attribution Maps which measures the cross-attention from tokens in the language condition to the UNet. Specifically, we used the improved DAAM-i2i guided heatmap variant (Tang et al., 2022; Chowdhury, 2024) which improves object localization. We observe that unrelated articles like "a", and "the" and possessive determiners like "his", "her", "our", "their" are not typically localized to a specific object, but rather have attribution maps diffuse over the background or various objects in the image. While similar phenomena has been noted in ViTs (Darcet et al., 2023) and pure text LLMs (Clark et al., 2019; Kovaleva et al., 2019; Xiao et al., 2023), our observation is novel in that text-to-image diffusion models are encoding contextual information in these "filler" words. For



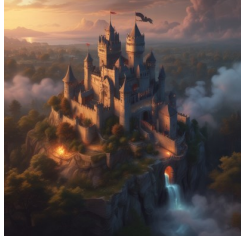
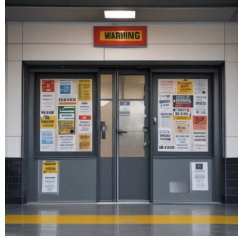
270 271 272 273 274 275 276 277	Image				
278 279 280 281 282 283 284	Raw prompt	Rusty suit of armor, portrait, glowing aura around it, damaged, inside a dark dungeon, fantasy setting, menacing, scratches, holes.	blue dog, painting, landscape, realistic, art	small medieval castle after battle, small medieval castle after battle, smoke, nighttime, birdseye view, style: magic the gathering	hospital close que to lockdown, hospital gaate wrap with a warning labels.
285 286 287 288 289 290 291 292 293	LLM caption	Portrait of a <u>rusty suit</u> of <u>armor</u> in a <u>dark fantasy dungeon</u> . A <u>menacing glowing aura</u> surrounds as it bears <u>scratches</u> and <u>holes</u> from <u>battle</u> , creating a <u>menacing presence</u> .	Realistic painting of a <u>blue dog</u> in a <u>landscape</u> .	<u>Bird's-eye view</u> of a <u>small medieval castle</u> after a <u>battle, smoke</u> rising from the <u>grounds</u> as night falls. Style: Magic the Gathering.	Close-up shot of a <u>hospital entrance</u> wrapped with <u>warning labels</u> during <u>lockdown</u> .

Figure 4: **Example of SDXL generated images from the captions, raw user prompts and LLM processed captions.** Raw prompts from users often contain typos or take the form of a non-natural language tag-like format. We instruct an LLM to transform the prompts into a natural language caption. **Noun chunks** (bolded and underlined) are derived from dependency parsing. Images are generated from the captions, with diffusion attribution maps recorded for the noun chunks.

effective localization, we remove articles and possessive determiners if they are the first word of a noun chunk.

4 EXPERIMENTS

We first evaluate the CLIP similarity between the generated images and the captions, and further characterize the safety and length of the captions. We then explore the semantic distribution of the images and the captions using CLIP, and visualize the spatial distribution of objects in a scene using diffusion attribution maps. Finally, we evaluate the performance of captioning and open-set segmentation models on our dataset. These characterizations demonstrate how StableSemantics can be a promising dataset for advancing visual semantic understanding. The data will be released under a CC0 1.0 license.

4.1 DATASET CHARACTERIZATION

After deduplication and LLM NSFW filtering, we have 224 thousand natural language captions. We evaluate the similarity of the SDXL-lightning generated images and the captions in Figure 3a using OpenAI’s CLIP ViT-B/16 (Radford et al., 2021). We find that the CLIP similarity peaks at 0.34, which is similar to CLIP scores achieved using SDXL. These scores typically range from 0.2 to 0.5 which means that our prompts and images can be interpreted to be semantically very similar given the higher range of scores. We visualize the token length of the captions in Figure 3b. Note that we do not generate images for captions exceeding 77 tokens post-padding. This yields a total of 200k captions which are used for image generation. In Figure 3c, we plot the NSFW scores of the captions used for image generation, as evaluated using the state-of-the-art Meta Llama Guard 2 model. We define the unsafe categories to the 3 official categories relating to sexual content, and the 1 official category related to hate speech. The scores are the “unsafe” softmax outputs between the “safe” and “unsafe” tokens. We find that the captions used for generation are overwhelmingly safe. In Figure 4, we provide examples of the images, the original human generated prompts which may often contain

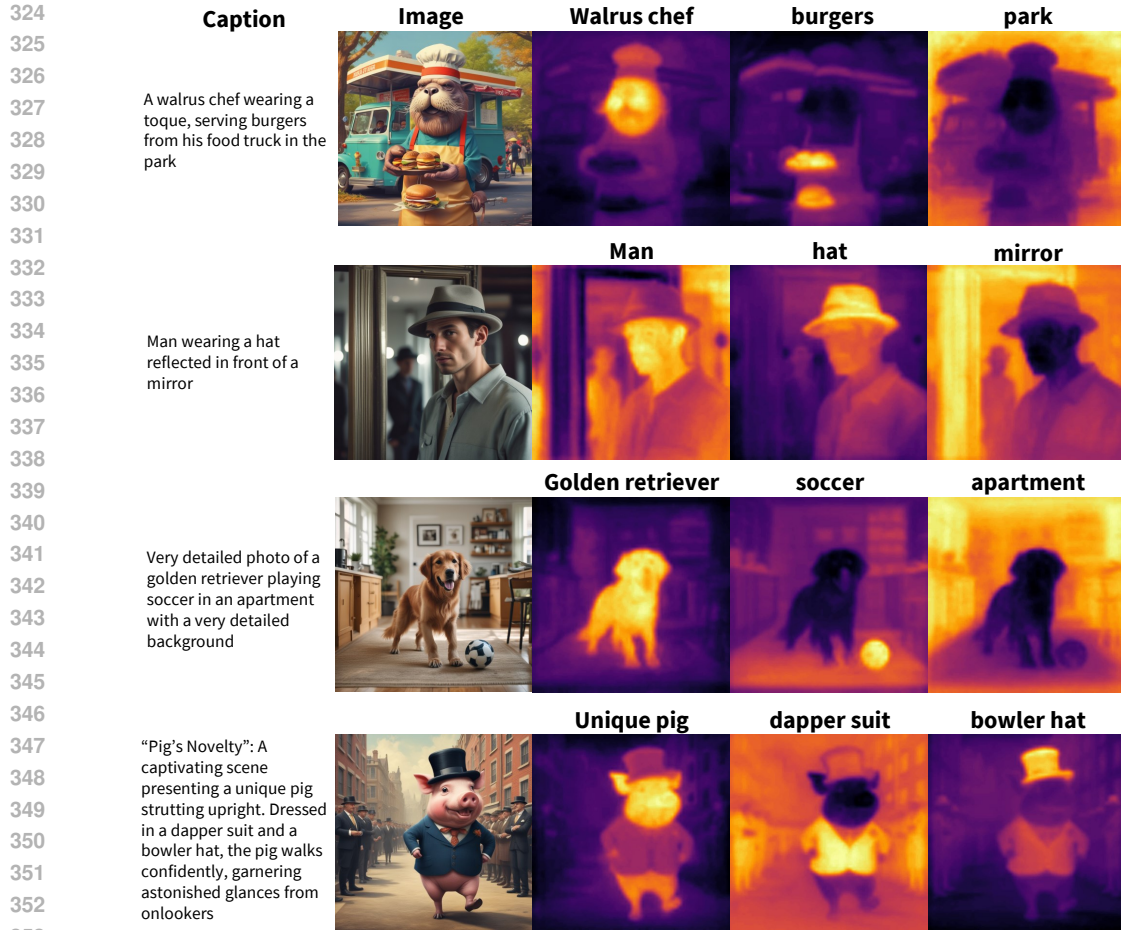


Figure 5: **Visualization of the dataset.** We show example captions used for image generation, images generated from the captions, and select noun chunks and their corresponding attention attribution maps. We find that our dataset contains accurate localizations for different semantic concepts.

typos or tags, and the LLM output natural language prompts. Likely due to human preference, we observe a higher ratio of images with visually interesting compositions.

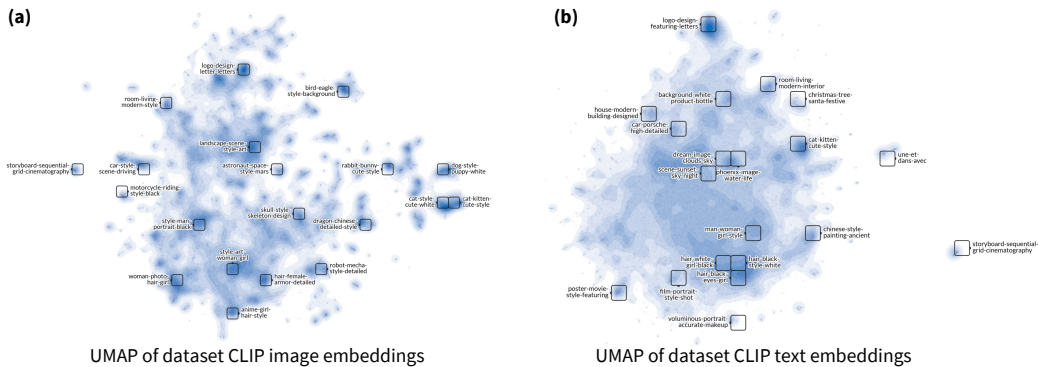


Figure 6: **UMAP visualization of dataset CLIP embeddings.** We use OpenAI CLIP ViT-B/16 to compute embeddings for both the generated (a) images and the (b) text. UMAP with the cosine metric is used to perform dimensionality reduction. We observe that images describing people, scenes, text, and animals occur with high frequency.

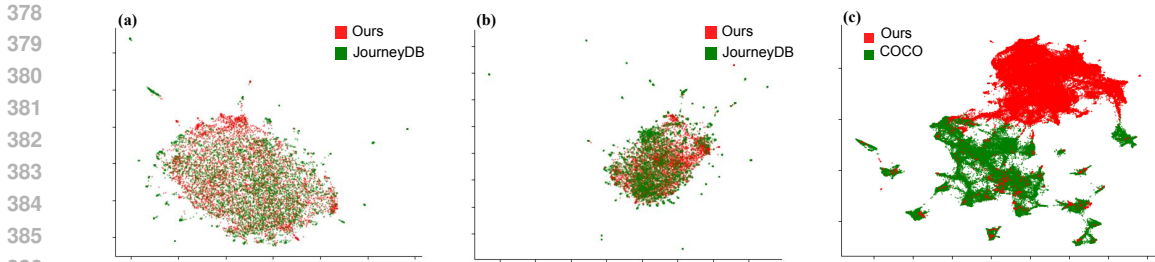


Figure 7: UMAP visualization of CLIP embeddings of different datasets. (a) CLIP text embeddings of the natural language captions. (b) CLIP text embeddings of the prompts. (c) CLIP image embeddings of StableSemantics against COCO.

Model	GPT-2	Llama 3 8B
DiffusionDB	335.86	92.02
JourneyDB	241.39	94.85
StableSemantics	206.26	91.41

Model	GPT-2	Llama 3 8B
JourneyDB	92.11	46.94
StableSemantics	87.35	43.74

Figure 8: Perplexity scores for prompts

Figure 9: Perplexity scores for captions

In table 8 we evaluate the prompts which are typically not natural language. For JourneyDB and StableSemantics we use the processed prompts (with parameters removed via regex). StableSemantics prompts consistently have lower perplexity than other datasets, likely due to human preference. A lower perplexity score indicates the prompt can be better predicted by the model and is more similar to natural language. Note that we do not use instruct-tuned models. Similarly, in table 9 we evaluate the captions which are LLM-processed prompts. Note that DiffusionDB did not provide captions. Captions from StableSemantics consistently have lower perplexity. This is likely due to using a more powerful LLM (Gemini vs GPT-3.5) and the human preference as a source of the raw captions.

4.2 SEMANTIC EXPLORATION OF THE DATASET

In Figure 6 we visualize the semantic distribution of whole images and the captions used to generate the images. We utilize UMAP (McInnes et al., 2018) with a cosine metric applied to CLIP embeddings for this visualization with wizmap (Wang et al., 2023c). We find that the distribution of both images and text exhibit peaks in concepts such as people, scenes, text, and animals (cats and dogs). These peaks likely reflect the effect of human preference on visually interesting images.

We compare the distribution of prompts, captions, and images against JourneyDB and COCO. Figure 7a shows that our captions (natural language outputs of Gemini/GPT) are a subset of JourneyDB’s captions. Figure 7b further shows that this cannot be due to the choice of LLM, and instead this is the influence of human preference for visually appealing images as human preferred prompts tile the broader prompt distribution, and do not form a linearly separable set. Figure 7c shows that image distribution of COCO and Our dataset is different and highlights that our dataset has images with objects in complex or imaginative scenarios not observed in real datasets.

The semantic maps we provide in our dataset help localize image regions corresponding to specific noun chunks from the prompts. In Figure 5 we visualize the captions used from image generation, the generated RGB image, and attention attribution masks corresponding to noun chunks shown in bold. We find that our dataset can provide semantic attributions that are well aligned to objects in the scene. This is likely due to the nature of Stable Diffusion, which leverages cross-attention guidance to generate complex compositional images.

We use these maps to analyze whether our images exhibit a trend of certain concepts being generated in specific regions on average. In Figure 10 we aggregate the masks of the top 100 noun chunks that have the highest CLIP similarity scores with concepts of interest. We apply this similarity-based matching to allow for inexact matching. Figure 10 clearly shows that the spatial distribution of concepts can be highly non-uniform. This bias likely reflects the distribution of concepts in natural

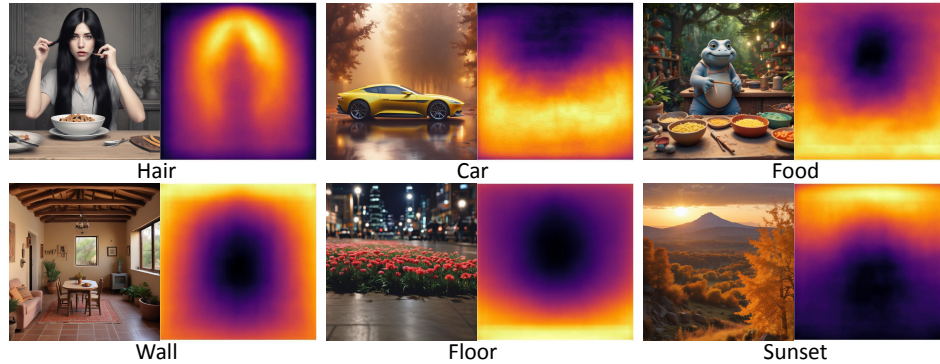


Figure 10: **Spatial distribution of semantic concepts.** For each concept, we visualize an example image containing the concept, as well as the spatial distribution averaged over occurrences. We utilize CLIP text similarity to select the top-100 most similar noun chunks and average those occurrences.

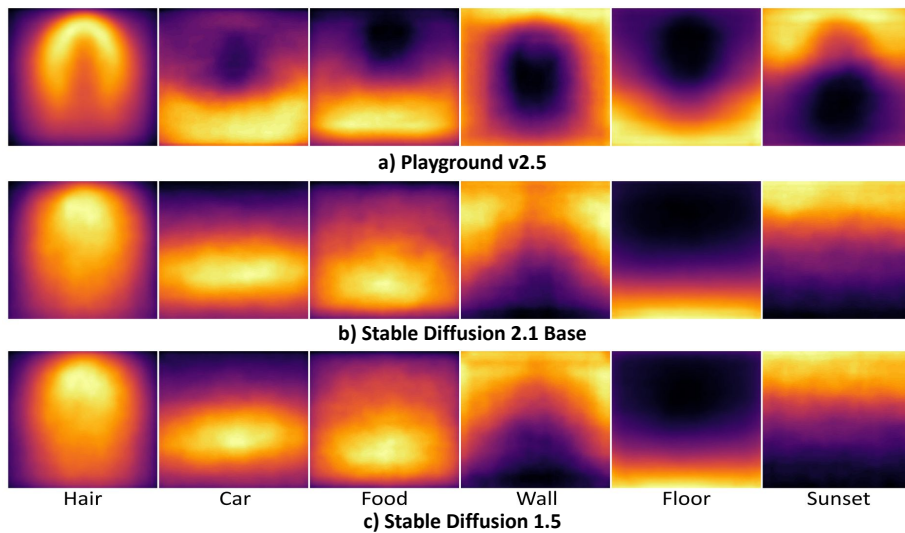


Figure 11: **Spatial distribution of semantic concepts for other generative models.**

images (Torralla & Oliva, 2003; Greene, 2013). For instance, it makes sense for the sunset to always be on the top, the walls towards the sides, and the floor towards the bottom. It is also very common to find human beings as the primary subjects in images which explains the placement of hair surrounding a central region. Finally, many images exhibit food on top of a table and cars on roads. In these scenarios, these semantic concepts typically occupy the bottom half of the visual field. Furthermore, we compare the spatial distribution of concepts across various popular generative models in Figure 11 and find similar trends being followed with slight variations. We visualize the frequency distribution of nouns grouped by wordnet hierarchy in Figure 12. Our dataset could be used to understand the spatial and visual bias present in natural images.

4.3 EVALUATION OF MODELS

In this section we evaluate the performance of state-of-the-art open-vocabulary image segmentation and captioning models on our dataset. For open-vocabulary segmentation methods, we evaluate the standard mean Intersection over Union (mIOU), where discrete masks are computed by taking the argmax over all noun chunks' continuous masks for a given prompt. As these methods also produce soft masks, we also evaluate the pearson correlation of the attribution maps from our datasets. In Table 14, We find that recent open-vocabulary segmentation models which modify CLIP (LSeg (Li et al., 2022), SCLIP (Wang et al., 2023a)) or leverage text-to-image diffusion models (ODISE (Xu et al., 2023)) perform better than their peers like MaskCLIP (Dong et al., 2023) CLIPSeg (Lüddecke & Ecker, 2022) and OVSeg (Liang et al., 2023).

486
487
488
489
490
491
492
493
494
495
496
497
498
499
500
501
502
503
504
505
506
507
508
509
510
511
512
513
514
515
516
517
518
519
520
521
522
523
524
525
526
527
528
529
530
531
532
533
534
535
536
537
538
539

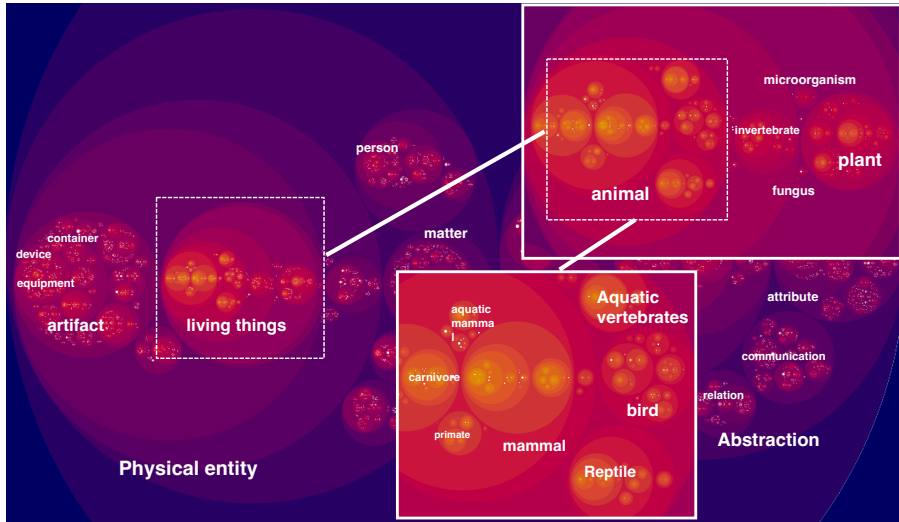


Figure 12: **Frequency of nouns visualized with wordnet hierarchy.** We parse the sentences and extract the nouns. The hierarchy is from wordnet Fellbaum (2010). The circle size corresponds to frequency.

Methods	E5-Mistral \uparrow	BLEU \uparrow	CIDEr \uparrow
LLaVA	67.9	1.2	3.1
BLIP-2	70.9	1.9	10.2
GIT	63.3	1.0	6.8
CoCa	66.8	1.7	9.7

Figure 13: **Performance comparison of captioning models.** We apply captioning models and evaluate the alignment of the outputs against the captions used to generate the images.

Method	mIoU \uparrow	Pearson \uparrow
MaskCLIP	0.015	0.199
SCLIP	0.109	0.236
LSeg	0.164	0.032
CLIPSeg	0.133	0.143
ODISE	0.096	0.300
OVSeg	0.035	0.181

Figure 14: **Performance comparison of open-set segmentation models.** We evaluate the IoU and Pearson correlation for noun chunks against model outputs.

We perform an experiment to finetune MaskCLIP (using the ViT-B/16 as backbone, initialized from laion2b_s34b_b88k weights) on a subset of our dataset using a cosine distance loss between the dense predicted output and the argmax-assigned spatial CLIP text embeddings. The training set is disjoint from the test set. Images are only selected for training/testing if they include three or more noun chunks. The Pearson correlation of the finetuned model increases from 0.199 (original MaskCLIP) to 0.38 (finetuned model).

We also evaluate recent vision-language models like LLaVA (Liu et al., 2024), BLIP-2 (Li et al., 2023), GIT (Wang et al., 2022a) and CoCa (Yu et al., 2022). for image captioning in Table 13. We evaluate the generated captions against the original captions using state-of-the-art E5-Mistral (Wang et al., 2023b) model to evaluate cosine similarity ($\times 100$ for clarity), BLEU-4 (Papineni et al., 2002), and CIDEr (Vedantam et al., 2015) scores. These results suggest that while the captions predicted by models may use different wording from the original caption, they can be semantically very similar.

5 DISCUSSION

Limitations and Future Work. Our work relies on human-submitted prompts, which may exhibit non-natural semantic co-occurrences. During the data collection process, we also observed a strong shift in the semantic distribution of prompts and images around holidays (Thanksgiving, Christmas). This suggests that continual data collection is required to mitigate bias.

Conclusion. We introduce StableSemantics, the first large-scale dataset that combines natural language captions, synthetic images, and diffusion attribution maps. Our work goes beyond prior datasets by providing spatially localized noun chunk to image region mappings. We explore the semantic distribution of whole images and objects within an image. The availability of this dataset will allow for the use of synthetic visual data in additional domains.

REFERENCES

- 540
541
542 Aishwarya Agrawal, Jiasen Lu, Stanislaw Antol, Margaret Mitchell, C. Lawrence Zitnick, Devi Parikh,
543 and Dhruv Batra. Vqa: Visual question answering. *International Journal of Computer Vision*, 123:
544 4 – 31, 2015. URL <https://api.semanticscholar.org/CorpusID:3180429>. 3
- 545
546 Yousef Alqasrawi. Bridging the gap between local semantic concepts and bag of visual words
547 for natural scene image retrieval. *ArXiv*, abs/2210.08875, 2016. URL <https://api.semanticscholar.org/CorpusID:63956645>. 1
- 548
549 Memoona Aziz, Umair Rehman, Muhammad Umair Danish, and Katarina Grolinger. Global-local
550 image perceptual score (glips): Evaluating photorealistic quality of ai-generated images. *arXiv*
551 *preprint arXiv:2405.09426*, 2024. 2
- 552
553 Björn Barz and Joachim Denzler. Content-based image retrieval and the semantic gap in the deep
554 learning era. *ArXiv*, abs/2011.06490, 2020. URL <https://api.semanticscholar.org/CorpusID:226306702>. 1
- 555
556 Andrew Brock, Jeff Donahue, and Karen Simonyan. Large scale gan training for high fidelity natural
557 image synthesis. *arXiv preprint arXiv:1809.11096*, 2018. 3
- 558
559 Clemens-Alexander Brust and Joachim Denzler. Not just a matter of semantics: the relationship
560 between visual similarity and semantic similarity. *arXiv preprint arXiv:1811.07120*, 2018. 1
- 561
562 Mathilde Caron, Hugo Touvron, Ishan Misra, Hervé Jégou, Julien Mairal, Piotr Bojanowski, and
563 Armand Joulin. Emerging properties in self-supervised vision transformers. In *Proceedings of the*
IEEE/CVF international conference on computer vision, pp. 9650–9660, 2021. 1
- 564
565 Rishi Dey Chowdhury. Daam-image2image, 2024. URL <https://github.com/RishiDarkDevil/daam-i2i>. 5
- 566
567 Kevin Clark, Urvashi Khandelwal, Omer Levy, and Christopher D Manning. What does bert look at?
568 an analysis of bert’s attention. *arXiv preprint arXiv:1906.04341*, 2019. 5
- 569
570 Timothée Darcet, Maxime Oquab, Julien Mairal, and Piotr Bojanowski. Vision transformers need
571 registers. *arXiv preprint arXiv:2309.16588*, 2023. 5
- 572
573 Karan Desai, Gaurav Kaul, Zubin Aysola, and Justin Johnson. Redcaps: Web-curated image-text data
574 created by the people, for the people. *arXiv preprint arXiv:2111.11431*, 2021. 3
- 575
576 Laurent Dinh, David Krueger, and Yoshua Bengio. Nice: Non-linear independent components
577 estimation. *CoRR*, abs/1410.8516, 2014. URL <https://api.semanticscholar.org/CorpusID:13995862>. 3
- 578
579 Xiaoyi Dong, Jianmin Bao, Yinglin Zheng, Ting Zhang, Dongdong Chen, Hao Yang, Ming Zeng,
580 Weiming Zhang, Lu Yuan, Dong Chen, et al. Maskclip: Masked self-distillation advances
581 contrastive language-image pretraining. In *Proceedings of the IEEE/CVF Conference on Computer*
Vision and Pattern Recognition, pp. 10995–11005, 2023. 9
- 582
583 Jiali Duan and C.-C. Jay Kuo. Bridging gap between image pixels and semantics via supervision:
584 A survey. *ArXiv*, abs/2107.13757, 2021. URL <https://api.semanticscholar.org/CorpusID:236493168>. 1
- 585
586 Omar Elharrouss, Somaya Al-Maadeed, Nandhini Subramanian, Najmath Ottakath, Noor Almaadeed,
587 and Yassine Himeur. Panoptic segmentation: A review. *arXiv preprint arXiv:2111.10250*, 2021. 1
- 588
589 Zach Evans, Julian D Parker, CJ Carr, Zack Zukowski, Josiah Taylor, and Jordi Pons. Long-form
590 music generation with latent diffusion. *arXiv preprint arXiv:2404.10301*, 2024. 3
- 591
592 Hui Fang, Gary Kwok-Leung Tam, Rita Borgo, Andrew J Aubrey, Philip W Grant, Paul L Rosin,
593 Christian Wallraven, Douglas Cunningham, David Marshall, and Min Chen. Visualizing natural
image statistics. *IEEE Transactions on Visualization and Computer Graphics*, 19(7):1228–1241,
2012. 3

- 594 Christiane Fellbaum. Wordnet. In *Theory and applications of ontology: computer applications*, pp.
595 231–243. Springer, 2010. 10
- 596
- 597 Ahna R Girshick, Michael S Landy, and Eero P Simoncelli. Cardinal rules: visual orientation per-
598 ception reflects knowledge of environmental statistics. *Nature Neuroscience*, 14:926–932, 7 2011.
599 ISSN 1097-6256. doi: 10.1038/nn.2831. URL [http://www.nature.com/articles/nn.](http://www.nature.com/articles/nn.2831)
600 [2831](http://www.nature.com/articles/nn.2831). 3
- 601 Ian Goodfellow, Jean Pouget-Abadie, Mehdi Mirza, Bing Xu, David Warde-Farley, Sherjil Ozair,
602 Aaron Courville, and Yoshua Bengio. Generative adversarial nets. *Advances in neural information*
603 *processing systems*, 27, 2014. 3
- 604
- 605 Yash Goyal, Tejas Khot, Douglas Summers-Stay, Dhruv Batra, and Devi Parikh. Making the v in
606 vqa matter: Elevating the role of image understanding in visual question answering. *International*
607 *Journal of Computer Vision*, 127:398 – 414, 2016. URL [https://api.semanticscholar.](https://api.semanticscholar.org/CorpusID:8081284)
608 [org/CorpusID:8081284](https://api.semanticscholar.org/CorpusID:8081284). 3
- 609 Michelle R. Greene. Statistics of high-level scene context. *Frontiers in Psychology*, 4, 2013. doi:
610 10.3389/fpsyg.2013.00777. 9
- 611
- 612 Agrim Gupta, Lijun Yu, Kihyuk Sohn, Xiuye Gu, Meera Hahn, Li Fei-Fei, Irfan Essa, Lu Jiang,
613 and José Lezama. Photorealistic video generation with diffusion models. *arXiv preprint*
614 *arXiv:2312.06662*, 2023. 3
- 615 Hasan Abed Al Kader Hammoud, Hani Itani, Fabio Pizzati, Philip Torr, Adel Bibi, and Bernard
616 Ghanem. Synthclip: Are we ready for a fully synthetic clip training? *arXiv preprint*
617 *arXiv:2402.01832*, 2024. 3
- 618
- 619 William Harvey, Saeid Naderiparizi, and Frank Wood. Conditional image generation by conditioning
620 variational auto-encoders. In *International Conference on Learning Representations*, 2021. URL
621 <https://api.semanticscholar.org/CorpusID:249191864>. 3
- 622
- 623 Matthias Heiler and Christoph Schnörr. Natural image statistics for natural image segmentation.
624 *International Journal of Computer Vision*, 63:5–19, 2005. 3
- 625
- 626 Margaret M. Henderson, Michael J. Tarr, and Leila Wehbe. Low-level tuning biases in higher visual
627 cortex reflect the semantic informativeness of visual features. *Journal of Vision*, 23(4):8–8, 04
628 2023. ISSN 1534-7362. doi: 10.1167/jov.23.4.8. URL [https://doi.org/10.1167/jov.](https://doi.org/10.1167/jov.23.4.8)
629 [23.4.8](https://doi.org/10.1167/jov.23.4.8). 3
- 630
- 631 Alexander Hepburn, Valero Laparra, Raul Santos-Rodriguez, Johannes Ballé, and Jesús Malo. On the
632 relation between statistical learning and perceptual distances. *arXiv preprint arXiv:2106.04427*,
633 2021. 3
- 634
- 635 Alexander Hepburn, Valero Laparra, Raul Santos-Rodriguez, and Jesús Malo. Disentangling the link
636 between image statistics and human perception. *arXiv preprint arXiv:2303.09874*, 2023. 3
- 637
- 638 Jonathan Ho, William Chan, Chitwan Saharia, Jay Whang, Ruiqi Gao, Alexey Gritsenko, Diederik P
639 Kingma, Ben Poole, Mohammad Norouzi, David J Fleet, et al. Imagen video: High definition
640 video generation with diffusion models. *arXiv preprint arXiv:2210.02303*, 2022. 1, 3
- 641
- 642 Jie Hu, Linyan Huang, Tianhe Ren, Shengchuan Zhang, Rongrong Ji, and Liujuan Cao. You
643 only segment once: Towards real-time panoptic segmentation. In *Proceedings of the IEEE/CVF*
644 *Conference on Computer Vision and Pattern Recognition*, pp. 17819–17829, 2023. 1
- 645
- 646 Jinbin Huang, Chen Chen, Aditi Mishra, Bum Chul Kwon, Zhicheng Liu, and Chris Bryan. Asap:
647 Interpretable analysis and summarization of ai-generated image patterns at scale. *arXiv preprint*
arXiv:2404.02990, 2024. 2
- 648
- 649 Mengqi Huang, Zhendong Mao, Quang Wang, and Yongdong Zhang. Not all image regions matter:
650 Masked vector quantization for autoregressive image generation. *2023 IEEE/CVF Conference*
on Computer Vision and Pattern Recognition (CVPR), pp. 2002–2011, 2023. URL <https://api.semanticscholar.org/CorpusID:258841408>. 3

- 648 Tero Karras, Samuli Laine, and Timo Aila. A style-based generator architecture for generative
649 adversarial networks. In *Proceedings of the IEEE/CVF conference on computer vision and pattern
650 recognition*, pp. 4401–4410, 2019. 3
- 651
652 Diederik P. Kingma and Prafulla Dhariwal. Glow: Generative flow with invertible 1x1 convolutions.
653 *ArXiv*, abs/1807.03039, 2018. URL [https://api.semanticscholar.org/CorpusID:
654 49657329](https://api.semanticscholar.org/CorpusID:49657329). 3
- 655 Diederik P Kingma and Max Welling. Auto-encoding variational bayes. *arXiv preprint
656 arXiv:1312.6114*, 2013. 3
- 657
658 Yuval Kirstain, Adam Polyak, Uriel Singer, Shahbuland Matiana, Joe Penna, and Omer Levy.
659 Pick-a-pic: An open dataset of user preferences for text-to-image generation. In *Thirty-seventh
660 Conference on Neural Information Processing Systems*, 2023. URL [https://openreview.
661 net/forum?id=G5RwHpBUv0](https://openreview.net/forum?id=G5RwHpBUv0). 3
- 662 Ricardo Kleinlein, Alexander Hepburn, Raúl Santos-Rodríguez, and Fernando Fernández-Martínez.
663 Sampling based on natural image statistics improves local surrogate explainers. *arXiv preprint
664 arXiv:2208.03961*, 2022. 3
- 665
666 Olga Kovaleva, Alexey Romanov, Anna Rogers, and Anna Rumshisky. Revealing the dark secrets of
667 bert. *arXiv preprint arXiv:1908.08593*, 2019. 5
- 668 Ranjay Krishna, Yuke Zhu, Oliver Groth, Justin Johnson, Kenji Hata, Joshua Kravitz, Stephanie
669 Chen, Yannis Kalantidis, Li-Jia Li, David A. Shamma, Michael S. Bernstein, and Li Fei-Fei. Visual
670 genome: Connecting language and vision using crowdsourced dense image annotations. *Int. J.
671 Comput. Vision*, 123(1), may 2017. ISSN 0920-5691. doi: 10.1007/s11263-016-0981-7. URL
672 <https://doi.org/10.1007/s11263-016-0981-7>. 3
- 673 Doyup Lee, Chiheon Kim, Saehoon Kim, Minsu Cho, and Wook-Shin Han. Autoregressive image
674 generation using residual quantization. *2022 IEEE/CVF Conference on Computer Vision and Pat-
675 tern Recognition (CVPR)*, pp. 11513–11522, 2022. URL [https://api.semanticscholar.
676 org/CorpusID:247244535](https://api.semanticscholar.org/CorpusID:247244535). 3
- 677
678 Boyi Li, Kilian Q Weinberger, Serge Belongie, Vladlen Koltun, and René Ranftl. Language-driven
679 semantic segmentation. *arXiv preprint arXiv:2201.03546*, 2022. 9
- 680 Junnan Li, Dongxu Li, Silvio Savarese, and Steven Hoi. Blip-2: Bootstrapping language-image
681 pre-training with frozen image encoders and large language models. In *International conference
682 on machine learning*, pp. 19730–19742. PMLR, 2023. 10
- 683
684 Feng Liang, Bichen Wu, Xiaoliang Dai, Kunpeng Li, Yinan Zhao, Hang Zhang, Peizhao Zhang, Peter
685 Vajda, and Diana Marculescu. Open-vocabulary semantic segmentation with mask-adapted clip.
686 In *Proceedings of the IEEE/CVF Conference on Computer Vision and Pattern Recognition*, pp.
687 7061–7070, 2023. 9
- 688 Shanchuan Lin, Anran Wang, and Xiao Yang. Sdxl-lightning: Progressive adversarial diffusion
689 distillation. *arXiv preprint arXiv:2402.13929*, 2024. 5
- 690
691 Tsung-Yi Lin, Michael Maire, Serge J. Belongie, James Hays, Pietro Perona, Deva Ramanan, Piotr
692 Dollár, and C. Lawrence Zitnick. Microsoft coco: Common objects in context. In *European
693 Conference on Computer Vision*, 2014. URL [https://api.semanticscholar.org/
694 CorpusID:14113767](https://api.semanticscholar.org/CorpusID:14113767). 3, 5
- 695
696 Haotian Liu, Chunyuan Li, Qingyang Wu, and Yong Jae Lee. Visual instruction tuning. *Advances in
697 neural information processing systems*, 36, 2024. 10
- 698
699 Timo Lüddecke and Alexander Ecker. Image segmentation using text and image prompts. In
700 *Proceedings of the IEEE/CVF Conference on Computer Vision and Pattern Recognition (CVPR)*,
701 pp. 7086–7096, June 2022. 9
- 702
703 Troy Luhman and Eric Luhman. High fidelity image synthesis with deep vaes in latent space. *arXiv
preprint arXiv:2303.13714*, 2023. 3

- 702 Kenneth Marino, Mohammad Rastegari, Ali Farhadi, and Roozbeh Mottaghi. Ok-vqa: A visual
703 question answering benchmark requiring external knowledge. *2019 IEEE/CVF Conference on*
704 *Computer Vision and Pattern Recognition (CVPR)*, pp. 3190–3199, 2019. URL [https://api.
705 semanticscholar.org/CorpusID:173991173](https://api.semanticscholar.org/CorpusID:173991173). 3
- 706
707 Leland McInnes, John Healy, and James Melville. Umap: Uniform manifold approximation and
708 projection for dimension reduction. *arXiv preprint arXiv:1802.03426*, 2018. 8
- 709
710 Roey Mechrez, Itamar Talmi, Firas Shama, and Lihi Zelnik-Manor. Maintaining natural image
711 statistics with the contextual loss. In *Computer Vision—ACCV 2018: 14th Asian Conference on*
712 *Computer Vision, Perth, Australia, December 2–6, 2018, Revised Selected Papers, Part III 14*, pp.
713 427–443. Springer, 2019. 3
- 714
715 Mehdi Mirza and Simon Osindero. Conditional generative adversarial nets. *ArXiv*, abs/1411.1784,
716 2014. URL <https://api.semanticscholar.org/CorpusID:12803511>. 3
- 717
718 Long Ouyang, Jeffrey Wu, Xu Jiang, Diogo Almeida, Carroll Wainwright, Pamela Mishkin, Chong
719 Zhang, Sandhini Agarwal, Katarina Slama, Alex Ray, et al. Training language models to follow
720 instructions with human feedback. *Advances in neural information processing systems*, 35:27730–
27744, 2022. 4
- 721
722 Kishore Papineni, Salim Roukos, Todd Ward, and Wei-Jing Zhu. Bleu: a method for automatic
723 evaluation of machine translation. In Pierre Isabelle, Eugene Charniak, and Dekang Lin (eds.),
724 *Proceedings of the 40th Annual Meeting of the Association for Computational Linguistics*, pp.
725 311–318, Philadelphia, Pennsylvania, USA, July 2002. Association for Computational Linguistics.
doi: 10.3115/1073083.1073135. URL <https://aclanthology.org/P02-1040>. 10
- 726
727 Niki Parmar, Ashish Vaswani, Jakob Uszkoreit, Lukasz Kaiser, Noam M. Shazeer, Alexander Ku,
728 and Dustin Tran. Image transformer. In *International Conference on Machine Learning*, 2018.
729 URL <https://api.semanticscholar.org/CorpusID:3353110>. 3
- 730
731 Dustin Podell, Zion English, Kyle Lacey, Andreas Blattmann, Tim Dockhorn, Jonas Müller, Joe
732 Penna, and Robin Rombach. Sdxl: Improving latent diffusion models for high-resolution image
733 synthesis. *arXiv preprint arXiv:2307.01952*, 2023. 1, 3, 4
- 734
735 Max H. Quinn, Erik Conser, Jordan M. Witte, and Melanie Mitchell. Semantic image retrieval via
736 active grounding of visual situations. *2018 IEEE 12th International Conference on Semantic*
737 *Computing (ICSC)*, pp. 172–179, 2017. URL [https://api.semanticscholar.org/
CorpusID:4871106](https://api.semanticscholar.org/CorpusID:4871106). 1
- 738
739 Alec Radford, Jong Wook Kim, Chris Hallacy, A. Ramesh, Gabriel Goh, Sandhini Agarwal, Girish
740 Sastry, Amanda Askell, Pamela Mishkin, Jack Clark, Gretchen Krueger, and Ilya Sutskever.
Learning transferable visual models from natural language supervision. In *ICML*, 2021. 6
- 741
742 Rafael Rafailov, Archit Sharma, Eric Mitchell, Christopher D Manning, Stefano Ermon, and Chelsea
743 Finn. Direct preference optimization: Your language model is secretly a reward model. *Advances*
744 *in Neural Information Processing Systems*, 36, 2024. 4
- 745
746 Aditya Ramesh, Prafulla Dhariwal, Alex Nichol, Casey Chu, and Mark Chen. Hierarchical text-
747 conditional image generation with clip latents. *ArXiv*, abs/2204.06125, 2022. URL [https:
//api.semanticscholar.org/CorpusID:248097655](https://api.semanticscholar.org/CorpusID:248097655). 3
- 748
749 Ali Razavi, Aaron Van den Oord, and Oriol Vinyals. Generating diverse high-fidelity images with
750 vq-vae-2. *Advances in neural information processing systems*, 32, 2019. 3
- 751
752 Danilo Rezende and Shakir Mohamed. Variational inference with normalizing flows. In *International*
753 *conference on machine learning*, pp. 1530–1538. PMLR, 2015. 3
- 754
755 Robin Rombach, Andreas Blattmann, Dominik Lorenz, Patrick Esser, and Björn Ommer. High-
resolution image synthesis with latent diffusion models. In *Proceedings of the IEEE/CVF Confer-*
ence on Computer Vision and Pattern Recognition, pp. 10684–10695, 2022. 1, 3

- 756 Christoph Schuhmann, Romain Beaumont, Richard Vencu, Cade W Gordon, Ross Wightman, Mehdi
757 Cherti, Theo Coombes, Aarush Katta, Clayton Mullis, Mitchell Wortsman, Patrick Schramowski,
758 Srivatsa R Kundurthy, Katherine Crowson, Ludwig Schmidt, Robert Kaczmarczyk, and Jenia
759 Jitsev. LAION-5b: An open large-scale dataset for training next generation image-text models.
760 In *Thirty-sixth Conference on Neural Information Processing Systems Datasets and Benchmarks*
761 *Track*, 2022. URL <https://openreview.net/forum?id=M3Y74vmsMcY>. 3, 5
- 762 Jiaming Song, Chenlin Meng, and Stefano Ermon. Denoising diffusion implicit models. *arXiv*
763 *preprint arXiv:2010.02502*, 2020. 1, 3
- 764 Keqiang Sun, Junting Pan, Yuying Ge, Hao Li, Haodong Duan, Xiaoshi Wu, Renrui Zhang,
765 Aojun Zhou, Zipeng Qin, Yi Wang, Jifeng Dai, Yu Qiao, Limin Wang, and Hongsheng Li.
766 JourneyDB: A benchmark for generative image understanding. In *Thirty-seventh Conference*
767 *on Neural Information Processing Systems Datasets and Benchmarks Track*, 2023. URL
768 <https://openreview.net/forum?id=vfzXDRTcF4>. 3, 4, 5
- 769 Morgan B Talbot, Rushikesh Zawar, Rohil Badkundri, Mengmi Zhang, and Gabriel Kreiman. Tuned
770 compositional feature replays for efficient stream learning. *IEEE Transactions on Neural Networks*
771 *and Learning Systems*, 2023. 3
- 772 Raphael Tang, Linqing Liu, Akshat Pandey, Zhiying Jiang, Gefei Yang, Karun Kumar, Pontus
773 Stenertorp, Jimmy Lin, and Ferhan Ture. What the daam: Interpreting stable diffusion using cross
774 attention. *arXiv preprint arXiv:2210.04885*, 2022. 2, 5
- 775 Gemini Team, Rohan Anil, Sebastian Borgeaud, Yonghui Wu, Jean-Baptiste Alayrac, Jiahui Yu, Radu
776 Soricut, Johan Schalkwyk, Andrew M Dai, Anja Hauth, et al. Gemini: a family of highly capable
777 multimodal models. *arXiv preprint arXiv:2312.11805*, 2023. 5
- 778 Bart Thomee, David A. Shamma, Gerald Friedland, Benjamin Elizalde, Karl Ni, Douglas Poland,
779 Damian Borth, and Li-Jia Li. Yfcc100m: the new data in multimedia research. *Commun. ACM*, 59
780 (2):64–73, jan 2016. ISSN 0001-0782. doi: 10.1145/2812802. URL [https://doi.org/10.](https://doi.org/10.1145/2812802)
781 [1145/2812802](https://doi.org/10.1145/2812802). 3
- 782 Tristan Thrush, Ryan Jiang, Max Bartolo, Amanpreet Singh, Adina Williams, Douwe Kiela, and Can-
783 dace Ross. Winoground: Probing vision and language models for visio-linguistic compositionality.
784 In *Proceedings of the IEEE/CVF Conference on Computer Vision and Pattern Recognition*, pp.
785 5238–5248, 2022. 5
- 786 Yonglong Tian, Lijie Fan, Phillip Isola, Huiwen Chang, and Dilip Krishnan. Stablerep: Synthetic
787 images from text-to-image models make strong visual representation learners. *Advances in Neural*
788 *Information Processing Systems*, 36, 2024. 3
- 789 Alexander Tong, Nikolay Malkin, Guillaume Hugué, Yanlei Zhang, Jarrid Rector-Brooks, Kilian
790 Fatras, Guy Wolf, and Yoshua Bengio. Improving and generalizing flow-based generative models
791 with minibatch optimal transport. *arXiv preprint arXiv:2302.00482*, 2023. 3
- 792 Antonio Torralba and Aude Oliva. Statistics of natural image categories. 2003. 3, 9
- 793 Hugo Touvron, Thibaut Lavril, Gautier Izacard, Xavier Martinet, Marie-Anne Lachaux, Timothée
794 Lacroix, Baptiste Rozière, Naman Goyal, Eric Hambro, Faisal Azhar, et al. Llama: Open and
795 efficient foundation language models. *arXiv preprint arXiv:2302.13971*, 2023. 3
- 800 Aaron Van Den Oord, Oriol Vinyals, et al. Neural discrete representation learning. *Advances in*
801 *neural information processing systems*, 30, 2017. 3
- 802 A. van der Schaaf and J.H. van Hateren. Modelling the power spectra of natural images: Statistics
803 and information. *Vision Research*, 36(17):2759–2770, 1996. ISSN 0042-6989. doi: [https://doi.org/](https://doi.org/10.1016/0042-6989(96)00002-8)
804 [10.1016/0042-6989\(96\)00002-8](https://doi.org/10.1016/0042-6989(96)00002-8). URL [https://www.sciencedirect.com/science/](https://www.sciencedirect.com/science/article/pii/0042698996000028)
805 [article/pii/0042698996000028](https://www.sciencedirect.com/science/article/pii/0042698996000028). 3
- 806 Ramakrishna Vedantam, C Lawrence Zitnick, and Devi Parikh. Cider: Consensus-based image
807 description evaluation. In *Proceedings of the IEEE conference on computer vision and pattern*
808 *recognition*, pp. 4566–4575, 2015. 10
- 809

- 810 Vibashan VS, Shubhankar Borse, Hyojin Park, Debasmit Das, Vishal Patel, Munawar Hayat, and Fatih
811 Porikli. Possam: Panoptic open-vocabulary segment anything. *arXiv preprint arXiv:2403.09620*,
812 2024. 1
- 813
814 Feng Wang, Jieru Mei, and Alan Yuille. Sclip: Rethinking self-attention for dense vision-language
815 inference. *arXiv preprint arXiv:2312.01597*, 2023a. 9
- 816 Jianfeng Wang, Zhengyuan Yang, Xiaowei Hu, Linjie Li, Kevin Lin, Zhe Gan, Zicheng Liu, Ce Liu,
817 and Lijuan Wang. Git: A generative image-to-text transformer for vision and language. *arXiv*
818 *preprint arXiv:2205.14100*, 2022a. 10
- 819
820 Liang Wang, Nan Yang, Xiaolong Huang, Linjun Yang, Rangan Majumder, and Furu Wei. Improving
821 text embeddings with large language models. *arXiv preprint arXiv:2401.00368*, 2023b. 10
- 822 Peng Wang, Qi Wu, Chunhua Shen, Anthony Dick, and Anton van den Hengel. Fvqa: Fact-based
823 visual question answering. *IEEE Transactions on Pattern Analysis and Machine Intelligence*, 40
824 (10), 2018. doi: 10.1109/TPAMI.2017.2754246. 3
- 825
826 Zijie J. Wang, Evan Montoya, David Munechika, Haoyang Yang, Benjamin Hoover, and Duen Horng
827 Chau. DiffusionDB: A large-scale prompt gallery dataset for text-to-image generative models.
828 *arXiv:2210.14896 [cs]*, 2022b. URL <https://arxiv.org/abs/2210.14896>. 3, 4, 5
- 829
830 Zijie J Wang, Fred Hohman, and Duen Horng Chau. Wizmap: Scalable interactive visualization for
831 exploring large machine learning embeddings. *arXiv preprint arXiv:2306.09328*, 2023c. 8
- 832
833 Ao Xiang, Jingyu Zhang, Qin Yang, Liyang Wang, and Yu Cheng. Research on splicing image detec-
834 tion algorithms based on natural image statistical characteristics. *arXiv preprint arXiv:2404.16296*,
835 2024. 3
- 836
837 Guangxuan Xiao, Yuandong Tian, Beidi Chen, Song Han, and Mike Lewis. Efficient streaming
838 language models with attention sinks. *arXiv preprint arXiv:2309.17453*, 2023. 5
- 839
840 Jiarui Xu, Sifei Liu, Arash Vahdat, Wonmin Byeon, Xiaolong Wang, and Shalini De Mello. Open-
841 vocabulary panoptic segmentation with text-to-image diffusion models. In *Proceedings of the*
842 *IEEE/CVF Conference on Computer Vision and Pattern Recognition*, pp. 2955–2966, 2023. 1, 9
- 843
844 Zebin You, Xinyu Zhang, Hanzhong Guo, Jingdong Wang, and Chongxuan Li. Are image distributions
845 indistinguishable to humans indistinguishable to classifiers?, 2024. URL <https://arxiv.org/abs/2405.18029>. 2
- 846
847 Peter Young, Alice Lai, Micah Hodosh, and J. Hockenmaier. From image descriptions to visual
848 denotations: New similarity metrics for semantic inference over event descriptions. *Trans-*
849 *actions of the Association for Computational Linguistics*, 2:67–78, 2014. URL <https://api.semanticscholar.org/CorpusID:3104920>. 3
- 850
851 Jiahui Yu, Zirui Wang, Vijay Vasudevan, Legg Yeung, Mojtaba Seyedhosseini, and Yonghui Wu.
852 Coca: Contrastive captioners are image-text foundation models. *arXiv preprint arXiv:2205.01917*,
853 2022. 10
- 854
855 Mert Yuksekgonul, Federico Bianchi, Pratyusha Kalluri, Dan Jurafsky, and James Zou. When and
856 why vision-language models behave like bags-of-words, and what to do about it? In *The Eleventh*
857 *International Conference on Learning Representations*, 2022. 5
- 858
859 Rushikesh Zawar, Krupa Bhayani, Neelanjan Bhowmik, Kamlesh Tiwari, and Dhiraj Sangwan. Detect-
860 ing anomalies using generative adversarial networks on images. *arXiv preprint arXiv:2211.13808*,
861 2022. 3
- 862
863 Daniel Zoran. *Natural Image Statistics for Human and Computer Vision*. PhD thesis, Citeseer, 2013.
3

864
865
866
867
868
869
870
871
872
873
874
875
876
877
878
879
880
881
882
883
884
885
886
887
888
889
890
891
892
893
894
895
896
897
898
899
900
901
902
903
904
905
906
907
908
909
910
911
912
913
914
915
916
917

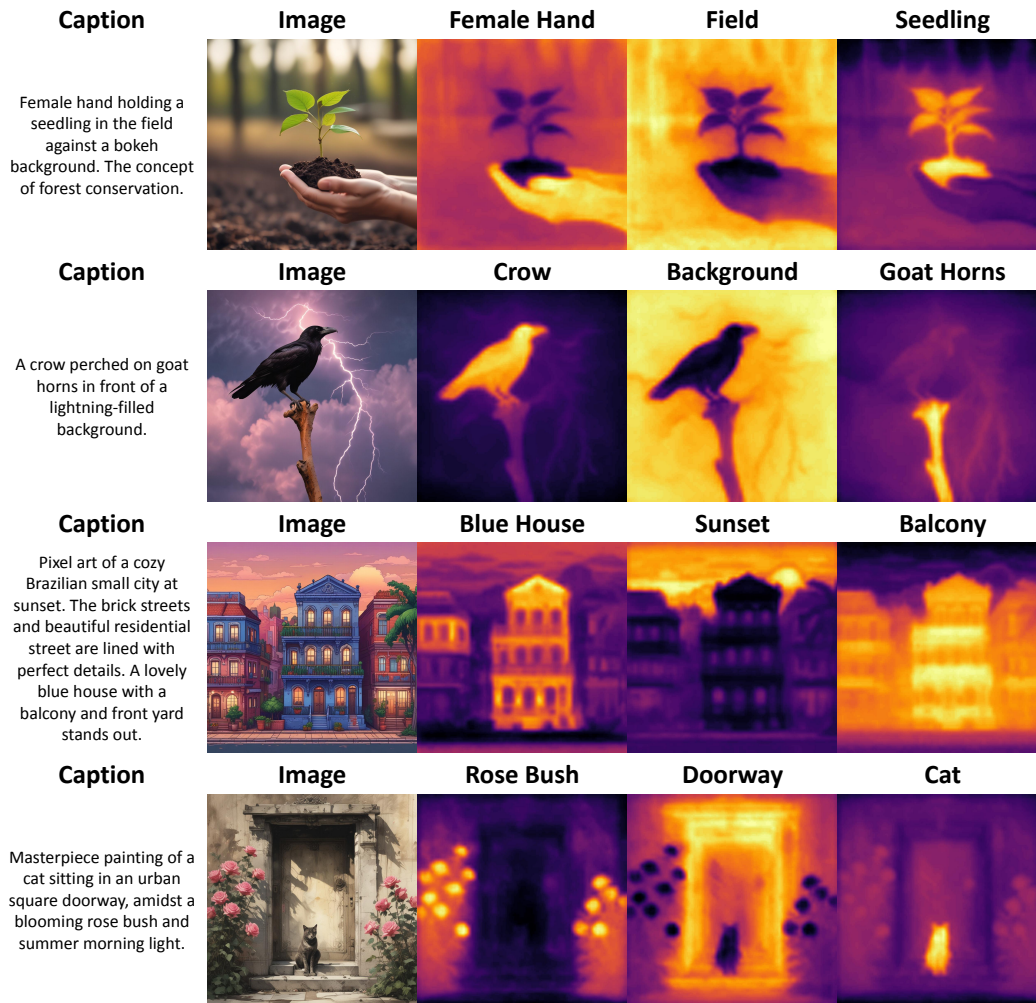
A APPENDIX

Sections

1. Additional dataset visualization (section [A.1](#))
2. Visualization of object distributions (section [A.2](#))
3. Comparison of open vocabulary segmentation methods (section [A.3](#))
4. Prompt used for language model cleanup of raw prompts (section [A.4](#))

A.1 ADDITIONAL DATASET VISUALIZATION

In this section, we provide additional visualizations of the natural language captions generated using a large language model from the raw user prompts, the RGB image, and semantic masks corresponding to select noun chunks in the image in Figure S.1 and Figure S.2.



957 **Figure S.1: Visualization of additional dataset examples.** We show the natural language caption
 958 used for the image generation, the image, and masks corresponding to select noun chunks.
 959
 960
 961
 962
 963
 964
 965
 966
 967
 968
 969
 970
 971

972
973
974
975
976
977
978
979
980
981
982
983
984
985
986
987
988
989
990
991
992
993
994
995
996
997
998
999
1000
1001
1002
1003
1004
1005
1006
1007
1008
1009
1010
1011
1012
1013
1014
1015
1016
1017
1018
1019
1020
1021
1022
1023
1024
1025

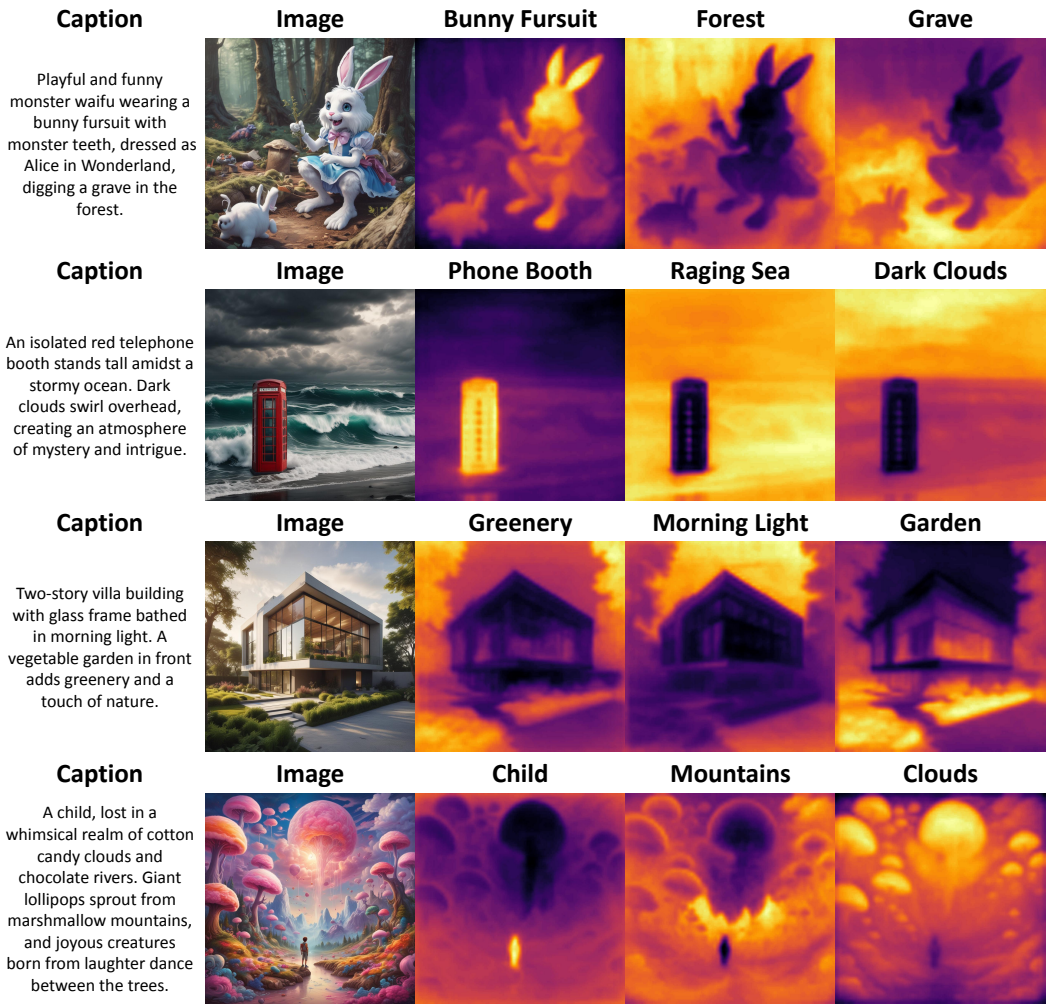
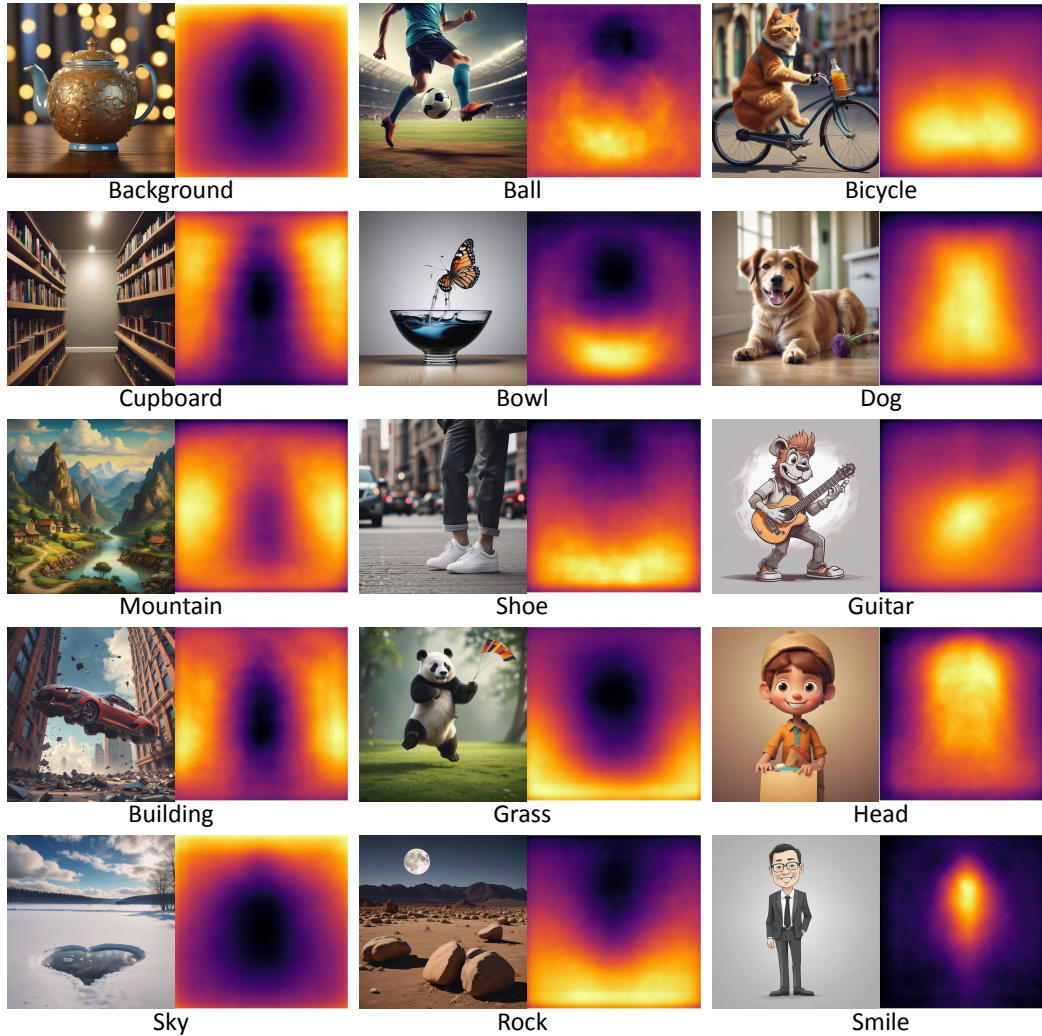


Figure S.2: **Visualization of additional dataset examples.** We show the natural language caption used for the image generation, the image, and masks corresponding to select noun chunks.

1026 A.2 VISUALIZATION OF OBJECT DISTRIBUTIONS
 1027

1028 In this section, we visualize the spatial distribution of various noun chunks in Figure S.3. We note
 1029 that several types of objects exhibit highly non-uniform spatial distributions.
 1030

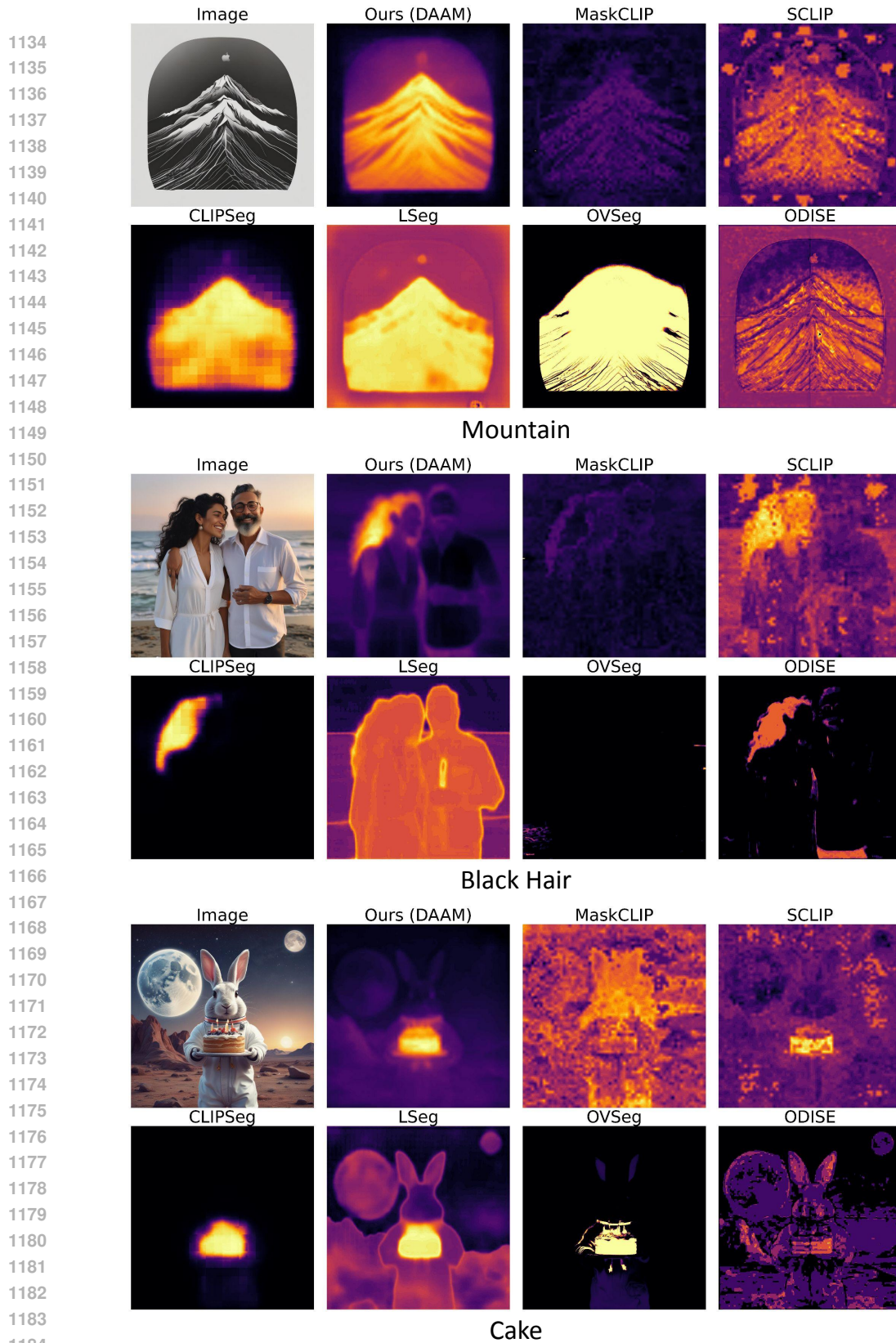


1065 **Figure S.3: Additional examples on the spatial distribution of concepts.** We provide additional ex-
 1066 amples of images containing a concept, and the average distribution of the top-100 images containing
 1067 the most similar noun chunks as evaluated using the CLIP text model.
 1068
1069
1070
1071
1072
1073
1074
1075
1076
1077
1078
1079

1080 A.3 COMPARISON OF OPEN VOCABULARY SEGMENTATION METHODS
1081

1082 In this section, we provide additional visualizations of the semantic maps from our dataset, and
1083 segmentation outputs in Figure S.4 and Figure S.5. We note that in general, the semantic masks in
1084 our dataset can accurately localize objects. However, there are specific cases (Lone Man) where the
1085 attention maps corresponding to noun chunks can include other contextual objects. We believe this
1086 occurs when the diffusion model tries to generate co-occurring scene and image parts that are not
1087 explicitly mentioned in the caption.

1088
1089
1090
1091
1092
1093
1094
1095
1096
1097
1098
1099
1100
1101
1102
1103
1104
1105
1106
1107
1108
1109
1110
1111
1112
1113
1114
1115
1116
1117
1118
1119
1120
1121
1122
1123
1124
1125
1126
1127
1128
1129
1130
1131
1132
1133



1186
1187

Figure S.4: Comparison of semantic maps and open vocabulary segmentation methods. We visualize the semantic attribution maps corresponding to noun chunks from our dataset, and the segmentation maps produced by various state-of-the-art methods.

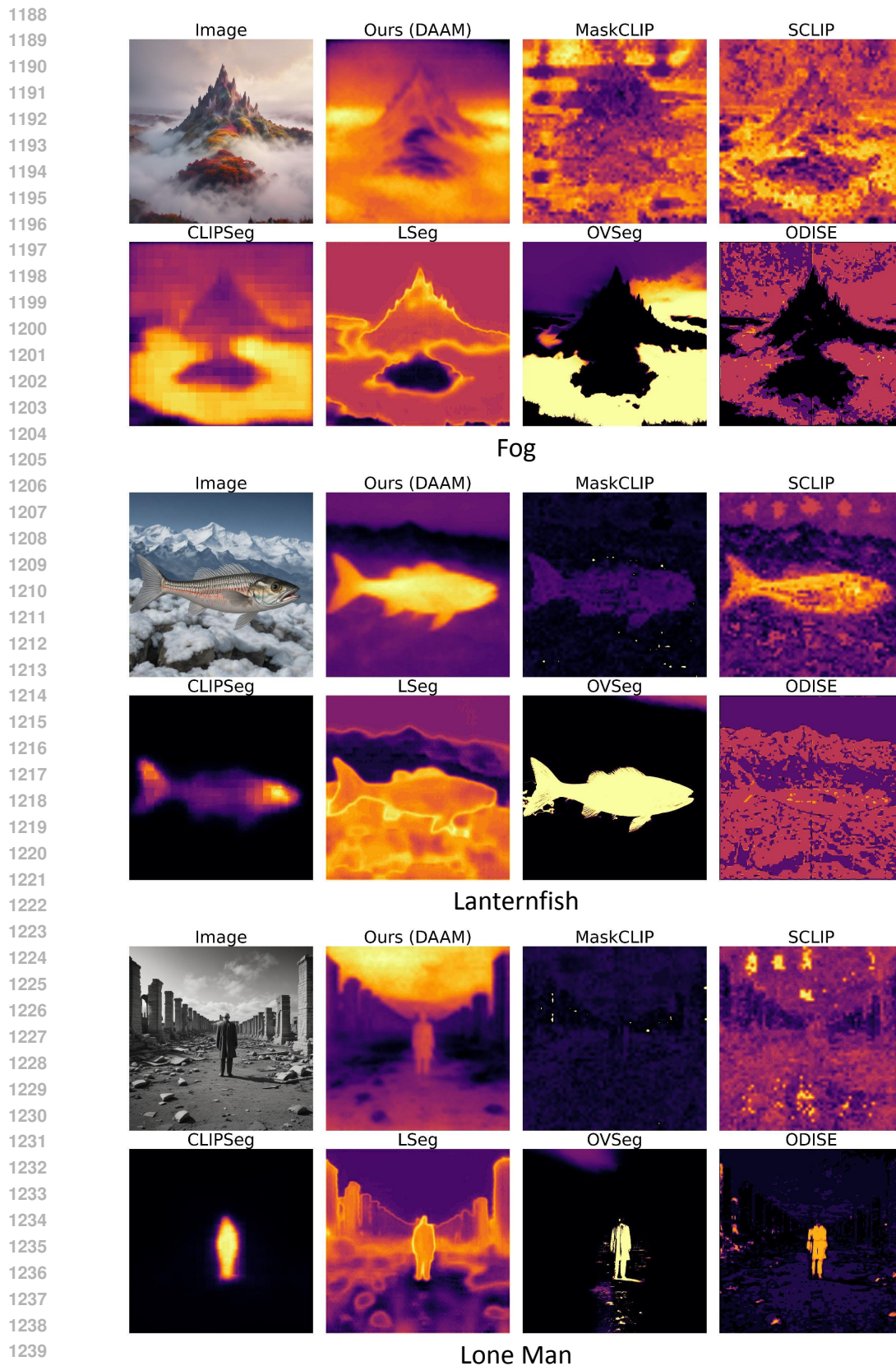


Figure S.5: Comparison of semantic maps and open vocabulary segmentation methods. We visualize the semantic attribution maps corresponding to noun chunks from our dataset, and the segmentation maps produced by various state-of-the-art methods. Note that the **Lone Man** illustrates how the semantic attribution maps can be imperfect. In this case it includes additional background.

1242 A.4 PROMPT USED FOR LANGUAGE MODEL CLEANUP OF RAW PROMPTS
1243

1244 We utilize the following prompt followed by the raw user prompt to obtain a natural language caption.
1245 Note that our raw prompts undergo simple `regex` based processing to remove some obvious errors
1246 before being provided to the language model.

1247
1248 You are going to be provided with the description of an image.
1249 You will transform and edit the description as needed into
1250 a cohesive natural language sentence or sentences without
1251 elaborating. If the original is mixed language, then your output
1252 should also be mixed language. Do not elaborate, do not provide
1253 information about people mentioned in the description.

1254 Make a best effort to use ALL WORDS AND DETAILS from the original
1255 description. DO NOT MAKE UP DETAILS unless absolutely necessary.
1256 BE AS CONCISE AS POSSIBLE, WHILE ATTEMPTING TO INCLUDE ALL WORDS
1257 AND DETAILS FROM THE ORIGINAL DESCRIPTION. You may only omit
1258 details or words if they are nonsensical or form a contradiction.
1259 Attempt to fix typos and remove invalid punctuation. Omit emojis
1260 in your output.

1261 When you output, use [START] before the output, and include [END]
1262 after the output. You may retain hash tags in the output only if
1263 hash tags were used in the original prompt. Here is the original
1264 description:
1265

1266
1267
1268
1269
1270
1271
1272
1273
1274
1275
1276
1277
1278
1279
1280
1281
1282
1283
1284
1285
1286
1287
1288
1289
1290
1291
1292
1293
1294
1295